ornl

OAK RIDGE NATIONAL LABORATORY

UNION CARBIDE

NUREG/CR-2752, Vol. 1
ORNL/TM-8365

Advanced Two-Phase Flow Instrumentation Program Quarterly Progress Report for January-March 1982

J. E. Hardy
S. C. Rogers
G. N. Miller
W. L. Zabriskie

Prepared for the U.S. Nuclear Regulatory Commission
Office of Nuclear Regulatory Research
Under Interagency Agreements DOE 40-551-75 and 40-552-75

OPERATED BY
UNION CARBIDE CORPORATION
FOR THE UNITED STATES
DEPARTMENT OF ENERGY

Printed in the United States of America. Available from
National Technical Information Service
U.S. Department of Commerce
5285 Port Royal Road, Springfield, Virginia 22161

Available from

GPO Sales Program
Division of Technical Information and Document Control
U.S. Nuclear Regulatory Commission
Washington, D.C. 20555

NUREG/CR-2752, Vol. 1
ORNL/TM-8365
Dist. Category R2

Contract No. W-7405-eng-26

Engineering Technology Division

ADVANCED TWO-PHASE FLOW INSTRUMENTATION PROGRAM QUARTERLY PROGRESS REPORT FOR JANUARY-MARCH 1982

J. E. Hardy G. N. Miller
S. C. Rogers W. L. Zabriskie

Manuscript Completed - June 15, 1982
Date Published - July 1982

Prepared for the
U.S. Nuclear Regulatory Commission
Office of Nuclear Regulatory Research
Under Interagency Agreements DOE 40-551-75 and 40-552-75

NRC FIN No. B0401

Prepared by the
OAK RIDGE NATIONAL LABORATORY
Oak Ridge, Tennessee 37830
operated by
UNION CARBIDE CORPORATION
for the
DEPARTMENT OF ENERGY

CONTENTS

ADVANCED TWO-PHASE FLOW INSTRUMENTATION PROGRAM QUARTERLY PROGRESS REPORT FOR JANUARY–MARCH 1982

J. E. Hardy G. N. Miller*
S. C. Rogers* W. L. Zabriskie*

ABSTRACT

The performance of the Westinghouse Reactor Vessel Level Indicating System (RVLIS) was analyzed for a series of tests in the Semiscale Test Facility. A summary of the results and conclusions from those small-break simulation experiments is presented. The Westinghouse RVLIS indicated a level measurement that was lower than the vessel coolant level for all tests. The RVLIS indication was at times higher than the vessel collapsed liquid level. This discrepancy was apparently created by structural differences in the Semiscale facility and a Westinghouse pressurized-water reactor (PWR). Modifications were made to Semiscale to better simulate a Westinghouse PWR, and a retest was completed. The RVLIS measurements showed much better agreement with the vessel collapsed liquid level for this retest.

In addition to the RVLIS analysis, an ultrasonic sensor is being developed to measure simultaneously the level, temperature, and density of the fluid in which it is immersed. The sensor is a thin, rectangular stainless steel ribbon, which acts as a waveguide and is housed in a perforated tube. The waveguide is coupled to a section of magnetostrictive material, which is surrounded by a pair of magnetic-coil transducers. These transducers are excited in an alternating sequence to interrogate the sensor with both torsional ultrasonic waves, using the Wiedemann effect, and extensional ultrasonic waves, using the Joule effect. The measured torsional wave transit time is a function of the density, level, and temperature of the fluid surrounding the waveguide. The measured extensional wave transit time is a function of the temperature of the waveguide only. The sensor is divided into zones by the introduction of reflecting surfaces at measured intervals along its length. Consequently, the transit times from each reflecting surface can be analyzed to yield temperature and density profiles along the length of the sensor. Improvements in acoustic wave dampener and transducer-sensor interface designs enhance the compatibility of the probe with high-temperature, high-radiation, water-steam environments and increase the likelihood of survival in such environments. Design and breadboard of a high-voltage pulser for driving the magnetic-coil transducer have resulted in an order of magnitude increase in signal strength. This increased signal

---

*Instrumentation and Controls Division.

strength is needed to improve signal-to-noise ratio and to ensure minimum attenuation of acoustic waves transmitted over long waveguides. Preliminary design is in progress for a new electronics package that will make multiple zone measurements faster and more flexible, allow output data to be displayed in real-time engineering units, and improve dynamic response, resolution, and accuracy.

---

1. INTRODUCTION

A variety of special instruments for measurements in high-temperature, high-pressure two-phase flow has been developed at the Oak Ridge National Laboratory (ORNL). One such recent activity has been the development of an ultrasonic sensor to measure the water level in the reactor vessel of a pressurized-water reactor (PWR).[1] Research has been sponsored by the U.S. Nuclear Regulatory Commission (NRC) Division of Accident Evaluation as a part of an effort to develop and implement improved instrumentation for use in PWRs to provide an unambiguous indication of the adequacy of core cooling. This advanced instrumentation must survive accident conditions and provide indications useful for postaccident analysis; it must also function properly under both natural- and forced-convection flow conditions.[2] Motivation for this effort stems from analyses of the accident at the Three Mile Island (TMI) nuclear power plant, during which a condition of low water level and inadequate core cooling was not recognized for an extended period, because no direct indication of water level in the reactor vessel existed.[3] Several concepts for satisfying these requirements have been proposed and are under development at ORNL and elsewhere. Continuing progress in the development of the ultrasonic sensor at ORNL has led to improved design and accuracy.

The ultrasonic level sensor is a promising long-term solution for monitoring core cooling adequacy, because it can display temperature and density profiles in addition to collapsed liquid and froth levels. Correlation of these outputs with those from other plant sensors would provide a self-checking capability for the probe. The ultrasonic sensor provides information relative to level, temperature, and density in continuous form, as opposed to sensors that simply indicate *full* or other discrete level points.[4,5] Compatibility with current reactor designs and the ability to perform under both normal reactor operating conditions (340°C, 17.2 MPa) and accident conditions are realized by the simple, all-metal construction of the sensor and by isolation of the transducer from the harsh environment of the reactor core. The remote location of electronics and absence of moving parts inside the reactor vessel make the probe very reliable and minimize maintenance requirements.

A measurement system was developed by Westinghouse to monitor in-vessel coolant levels by means of differential pressure (dP) cells covering selected ranges. This Reactor Vessel Level Indicating System (RVLIS) and its basic requirements and components were described previously.[6] Evaluation of the performance of the RVLIS for the upper-head injection (UHI) series (S-UT-3, S-UT-6, and S-UT-7) has been reported earlier.[7,8] A summary of the results for all the experiments, which included four UHI tests, three natural-circulation tests, a system time-response test, and one intermediate-break test is presented.

2. ULTRASONIC LEVEL SENSOR

2.1 Background Theory

The theory describing the magnetostrictive transduction of extensional and torsional ultrasonic waves and the propagation of these waves in thin waveguides may be found in the literature.[9-12] A brief summary of the basic principles may benefit those who are not acquainted with this application of ultrasonics.

Both extensional and torsional stress pulses can be generated in magnetostrictive materials by utilizing the Joule and Wiedemann effects, respectively.[9] A current pulse introduced into a coil surrounding a ferromagnetic rod creates a magnetic flux transient in the rod, which causes a change in its length (Joule effect). This sudden change in length generates an acoustic pulse that propagates as an extensional wave at the speed of sound within the material. A returning stress pulse generates a changing flux, by the Villari effect, that links the coil. This change in flux produces a voltage across the coil as a result of Faraday's law. The Wiedemann effect is a two-dimensional extension of the Joule effect. If a circumferential magnetic bias exists in the magnetostrictive rod, then an axially changing flux will twist the rod helically, initiating a shear stress pulse. This stress pulse propagates as a torsional wave, which, on its return, produces an output voltage by the inverse Wiedemann effect and Faraday's law.

In thin waveguides, acoustic pulses propagate as waves at a phase velocity of the general form

$$v = \sqrt{\frac{\text{stiffness term}}{\text{inertia term}}} \; . \qquad (1)$$

For a noncircular waveguide in a vacuum, the velocity of a dispersionless extensional wave is given by $v_e = \sqrt{E/\rho_s}$; for a dispersionless torsional wave, $v_t = K\sqrt{G/\rho_s}$. Young's modulus E and the shear modulus G represent the stiffness terms for each mode. The waveguide density ρ_s represents the inertia term for the extensional mode, whereas ρ_s and the waveguide shape factor K each contribute to the inertia term for the torsional mode. K is a function of the geometry of the waveguide.[10] An increase in temperature decreases both the stiffness and density terms. For stainless steel, the stiffness terms decrease at a much greater rate than the density term, resulting in a net decrease in acoustic velocity with an increase in temperature for each mode.

For a waveguide immersed in a fluid of density ρ the extensional wave velocity v_e remains essentially unchanged, while the torsional wave velocity becomes[11]

$$v_t = K\sqrt{\frac{G}{\rho_s}}\left[1 + \frac{\rho}{\rho_s}\left(1 - \frac{1}{K}\right)\right] , \; K < 1 \; . \qquad (2)$$

The noncircular geometry of the waveguide (quantified by K) allows coupling of inertia from the surrounding fluid to the waveguide. An additional inertia term caused by this coupling increases the effective inertia of the waveguide, thereby decreasing the torsional wave velocity [Eq. (1)].

The characteristic impedances as seen by an extensional wave and by a torsional wave are given by $Z_e = \rho_s v_e A$ and $Z_t = \rho_s v_t J$ respectively, where A is the cross-sectional area and J is the cross-sectional polar moment of inertia of the waveguide. The partial reflection of an incident wave at a boundary of the waveguide depends on the impedance match of adjacent sides. The reflection coefficient at the interface between two regions for a particular wave mode is given by

$$R_{1,2} = (Z_1 - Z_2)/(Z_1 + Z_2) .$$

Attenuation of the amplitude of an acoustic pulse results from the partial transmission of the incident wave's energy to an adjacent medium and from internal absorption losses.

A traveling acoustic wave pulse contains a broad, symmetrical spectrum of frequencies about a center frequency f_o. The relationship between the wavelength λ, frequency f, and velocity v of the traveling wave is expressed by $\lambda = v/f$. Dispersion, or the dependency of velocity on frequency, causes the pulse shape to spread out in time into many half cycles of pulse amplitude, an effect known as chirping. For dispersionless propagation, the ratio of waveguide diameter or width to wavelength must be kept below a critical value.[12] Typically, this value is 1:8.

2.2 Principle of Operation

The operation of the ultrasonic probe developed at ORNL for measuring the level, temperature, and density of the fluid in which it is immersed is based on the principles outlined in the previous section. The complete system consists of a sensor, a transducer, signal conditioning electronics, and a microcomputer (Fig. 1). The sensor is a rectangular waveguide housed in a perforated tube and coupled to a transducer by a lead-in waveguide through a transducer-sensor interface. The transducer consists of a 1.6-mm-diam section of magnetostrictive material surrounded by a pair of coils. The transducer is terminated by a back-length waveguide, which is fed into an impedance-matching acoustic wave dampener. The transducer coils are excited by the signal conditioning electronics, which both transmit and receive the signal pulses to provide data to the microcomputer for processing.

The electronics provide current pulses to each coil in an alternating sequence to launch extensional wave and torsional wave pulses in the magnetostrictive rod in each direction. The end echoes from the back-length are dampened so as not to interfere with the signals from the sensor. The forward-launched signals propagate in the waveguide through the transducer-sensor interface along the lead-in to the sensor. Incident waves are partially reflected at the interface of the lead-in and sensor,

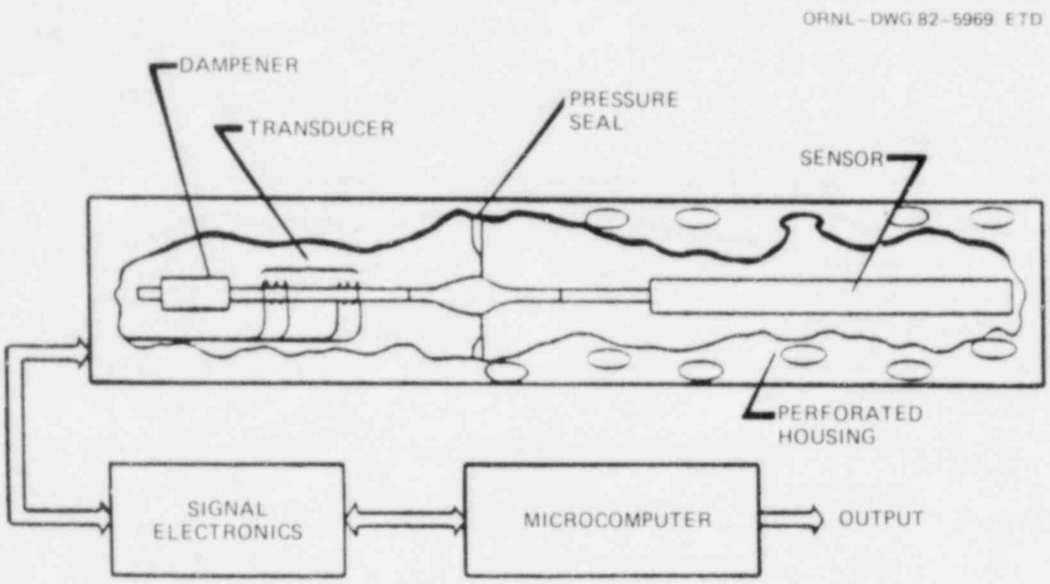

Fig. 1. Ultrasonic level detector system design.

at the sensor termination, and at any notches used to mark the zones along the length of the sensor; reflected pulses travel back to the transducer coils. There, they are converted to electrical signals, received by the signal conditioning electronics, and used to measure the round trip transit time of each wave in the sensor. The measured torsional transit time is a function of density, level, and temperature of the surrounding fluid. The measured extensional transit time is a function of the temperature component of the torsional signal. These signals are statistically sampled by the microcomputer and processed using algorithms that output level, temperature, and density.

2.3 Dampener

A nuclear-grade acoustic wave dampener has been developed to eliminate undesirable back end reflections of torsional and extensional waves from the waveguide. Dampening prevents these spurious echoes from interfering with signals of interest in the echo detection electronics. By the elimination of reverberations from the back-length termination, the pulse repetition rate may be increased. This increases the amount of information that can be gathered and improves time correlations between the torsional and extensional mode signals. Application of a dampener rather than a long back length (which causes back end reflections to return after the sensor echoes) results in the reduction of the probe length by more than a factor of two. This will facilitate installation by keeping the probe within dimensional constraints of current reactor designs.

Figure 2(a) illustrates the basic design of the dampener. The dampener consists of stainless steel wool that surrounds the waveguide and is sandwiched between two stainless steel brackets. Support screws may be

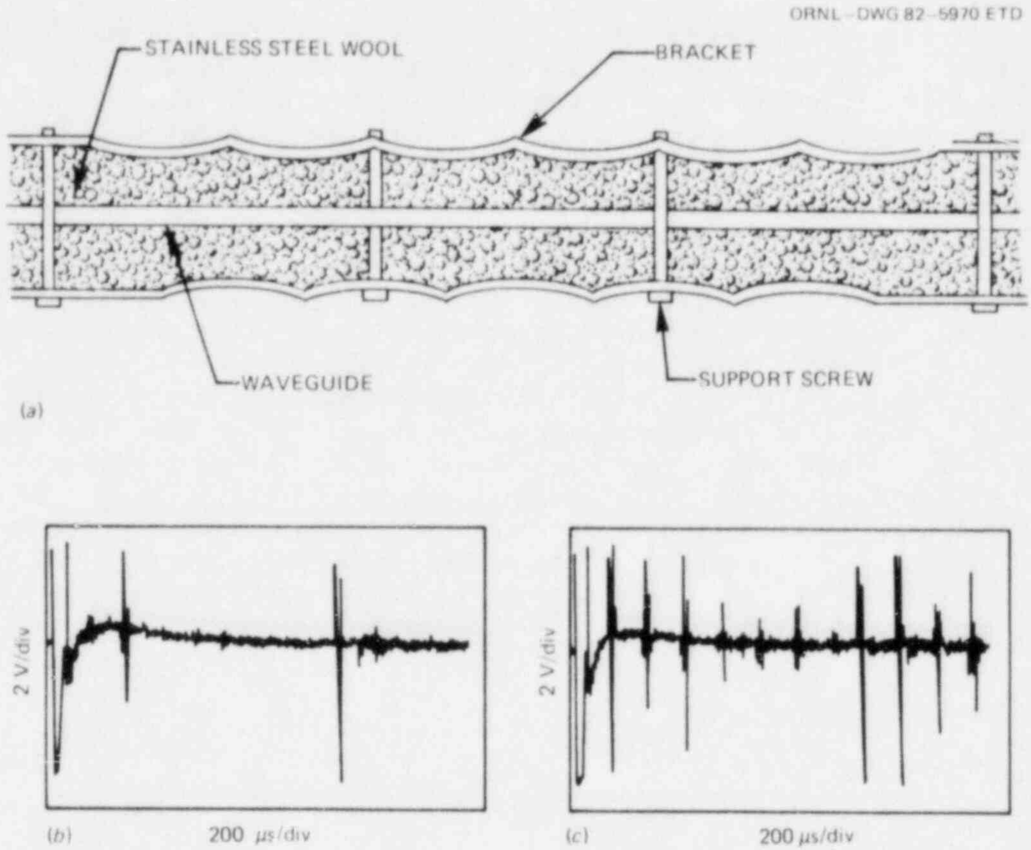

Fig. 2. Basic design of (a) acoustic wave dampener showing torsional signal (b) with dampener and (c) without dampener.

tightened to compress the stainless steel wool against the waveguide. This can be used to effectively tune the dampener until there is an impedance match between the dampener and the waveguide, allowing most of the acoustic wave energy to pass into the dampener from the waveguide. High internal absorption losses resulting from the inhomogeneous nature of the steel wool causes the acoustic waves to be greatly attenuated. An example of a torsional mode pulse train that includes end reflections is shown in Fig. 2(c). Figure 2(b) is the same signal with all the echoes, except those of interest, removed by the dampener.

2.4 Transducer-Sensor Interface

A disk-type waveguide penetration, which could isolate the probe's transducer from the sensor while allowing acoustic waves to pass between them, was designed by the authors and L. C. Lynnworth of Panametrics, Inc. Development of the design details and actual fabrication of the interface were carried out by Panametrics, and the interface was subsequently purchased by ORNL and installed on the probe. The interface protects the transducer from the high-temperature, high-pressure water-steam environment inside the reactor vessel and allows the magnetostrictive material to remain below the critical temperature necessary for the survival of the transducer (the magnetic bias of the magnetostrictive material vanishes at ~260°C). The interface is a 1.6-mm-thick disk that is machined to 0.13 mm at its center where an enlarged section of waveguide passes through [Fig. 3(a)].

This geometry makes the waveguide look massive in comparison with the disk, thus nearly matching their respective impedances. The reflection coefficient R is therefore small enough at the disk to allow transmission of most of the acoustic wave energy through the seal.

Figures 3(b) and 3(c) are oscillograms of extensional and torsional waves that were launched in a waveguide using the interface described in Fig. 3(a). Extensional waves are transmitted through the seal with virtually no reflections at the seal. Even though some acoustic energy of the torsional wave is reflected by the seal, an adequate amount of energy is transmitted. Some dispersion of the signal pulse is present in the torsional waves because of the large diameter of the waveguide at the disk. Continued development will address this problem.

ORNL-DWG 82-5971 ETD

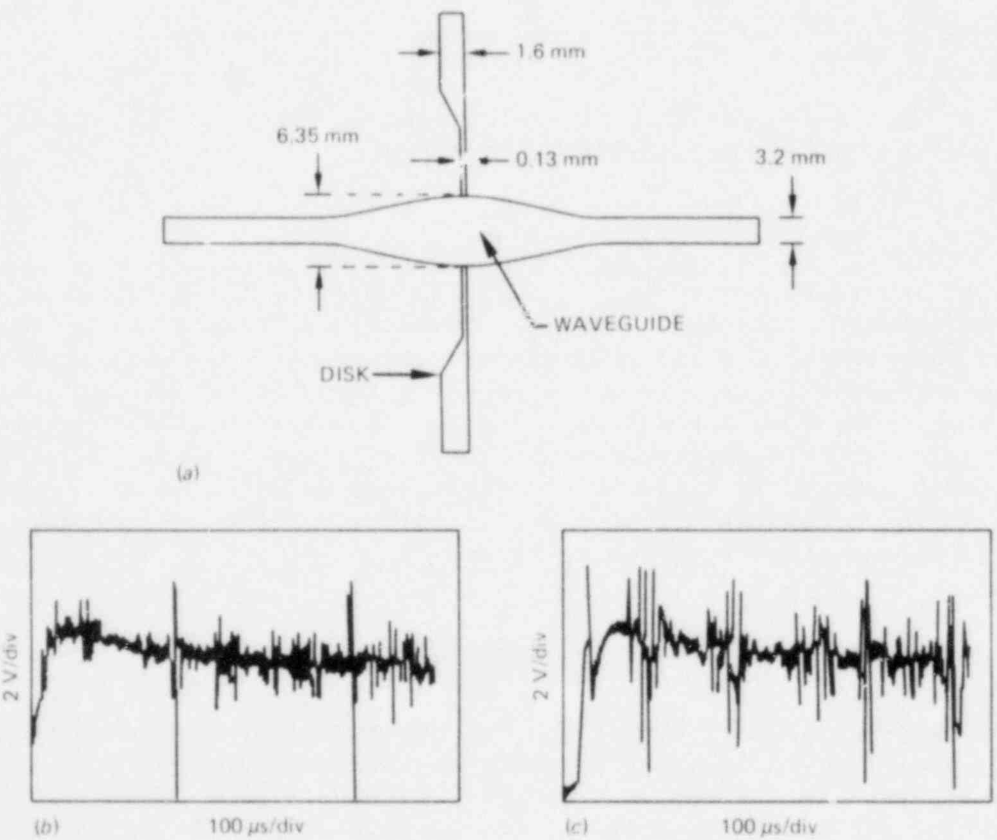

Fig. 3. Using the (a) interface of transducer and sensor, (b) extensional waves and (c) torsional waves were launched in a waveguide.

An alternative solution to the transducer-sensor interface problem may be to use a long, narrow restriction surrounding that section of waveguide. This restriction would reduce heat and moisture convection to the transducer without interfering with acoustic wave transmission because this interface would not physically contact the waveguide.

2.5 Electronics Design

Signal levels in the sensor are of particular interest for reactor vessel applications. High-energy acoustic signals are needed to minimize attenuation of acoustic waves transmitted over long waveguides, to offset the accumulative effect of partial energy reflection at an increased number of notches, and to maintain signal detectability in the presence of high noise levels found in a reactor vessel. Recent laboratory tests have shown that the acoustic signal amplitude can be increased significantly by using a more powerful drive circuit. For a 1.6-mm-diam waveguide, 12-mV peak-to-peak signal levels are obtained by using the 20-V dc drive output of the Panametrics Panatherm [Fig. 4(a)]. In Fig. 4(b), signal levels in the same waveguide approach 1.2 V peak-to-peak when a specially designed 300-V dc electronic drive circuit is used. Figure 4(c) shows 0.3-V peak-to-peak signal produced in a 3.2-mm-diam waveguide by the 300-V dc drive. For larger waveguide diameters, lower operating frequencies are needed to prevent dispersion and reduce attenuation caused by the establishment of standing waves in the waveguide.

Preliminary design of a new, complete electronics package has begun. The existing design philosophy uses three levels of operation: (1) hardwired circuits for signal generation and detection; (2) microprogrammed controller for direct control of these circuits and their associated high-speed timing components; and (3) embedded microcomputer for controller interaction, data acquisition, processing, and display; and (4) operator and peripheral interface. The hardwired components include the high-voltage pulser (previously mentioned); pulser drive and power supply receiver; pulser/receiver isolation switch, multiplexer, and echo amplifier; detector, blanking, and interval timer. The controller will sequence through a microprogram (firmware) to control interaction between various high-speed components such as blanking and interval timer and to manage flow of data between these components and the microcomputer through a buffer. By shifting the burden of high-speed control from the microcomputer to the microprogrammed controller, a medium-speed microcomputer may be used while maintaining flexibility in firmware. Speed is not compromised because the microcomputer can process data and drive other interfaces in parallel with the controller operation.

A primary candidate for the microcomputer is a single-board Z80-based computer manufactured by R. W. Electronics. This computer will run both 8080/8085 and Z80 programs and includes 72 parallel input/output (I/O) lines, keyboard controller, 12K EPROM, 2K RAM, 8 16-bit counter-timer channels, 2 serial I/O ports, and a high-speed arithmetic processor.

ORNL-DWG 82-5972 ETD

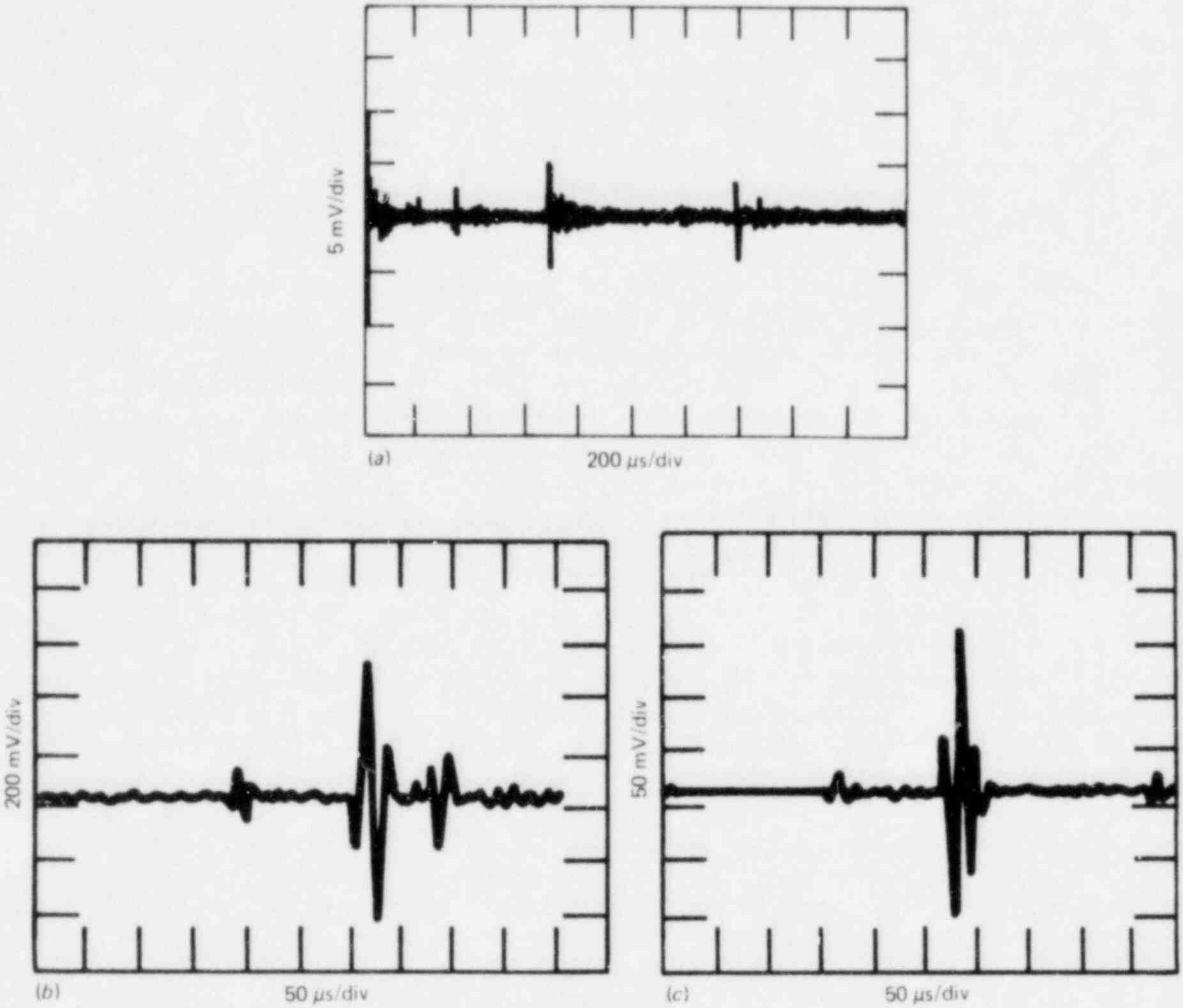

Fig. 4. Signal obtained with (a) commercial electronics, (b) special 300-V electronics, and (c) larger waveguide combined with 300-V electronics.

3. EVALUATION OF THE WESTINGHOUSE RVLIS

The Westinghouse RVLIS monitors the in-vessel liquid level by means of dP measurements. The Westinghouse RVLIS consisted of three dP cells with three pressure tap locations on the vessel: vessel top, hot leg, and vessel bottom. The three possible measurement spans were

1. from the vessel top to the hot leg, the upper-head sensor (WUPHLV);
2. from the vessel top to the bottom of the vessel level, the vessel level (WVESLV); and
3. from the bottom of the vessel to the top, a dynamic measurement for when coolant pumps are operating (WDVNLV).

The effectiveness of the RVLIS in monitoring in-vessel coolant levels was judged by comparison of the RVLIS data with data from a combination of Semiscale instruments that measure test vessel fluid density, flow, fluid temperatures, and dP over selected spans.

The definitions of two terms should be clarified. Collapsed liquid level is an equivalent water level in the vessel if all voids are collapsed (measured by a dP cell). The froth level is defined as the level at which an inflection occurs on a densitometer curve with the density decreasing sharply to a steam value.

The Westinghouse RVLIS was installed at Semiscale, and its performance was evaluated for the tests listed in Table 1. The RVLIS performance is evaluated in detail for each test in Refs. 7, 8, and 13. Only the conclusions will be presented in this section.

The conclusions of the analysis of the RVLIS performance are

1. In S-UT-3 and S-UT-6 tests the RVLIS indicated a lower level than the two-phase froth level. However, the RVLIS indications were as much as 200 cm above the vessel collapsed liquid level at times during the tests. This discrepancy was apparently related to the structural differences between the upper internals in Semiscale and a Westinghouse PWR. [Modifications were made to the Semiscale facility to better simulate the flow distribution of a Westinghouse PWR. A repeat test S-UT-8 was conducted (see conclusion 4)].

2. In the S-UT-7 test (UHI was used) the RVLIS measurement agreed well with the vessel collapsed liquid level, and the RVLIS level was well below the two-phase froth level.

3. The natural-circulation tests S-NC-2B, S-NC-3, and S-NC-8B results showed that the level indication by the RVLIS agreed well with the vessel collapsed liquid level and was always lower than the vessel two-phase froth level.

4. In S-UT-8 (a repeat of S-UT-6) the agreement between the RVLIS indication and the vessel collapsed liquid level was much improved over S-UT-3 and S-UT-6. The difference was reduced from as much as 200 cm to only ~30 cm for S-UT-8. The test results indicated that the modifications performed on the Semiscale facility enabled it to better simulate a Westinghouse PWR and, with the modifications, the RVLIS performed adequately.

5. The time-response test confirmed expected values derived from ORNL-developed dP system response equations and indicated that the RVLIS was fast enough for liquid-level detection.

Table 1. Semiscale tests with Westinghouse RVLIS

Test	Test type	References
S-UT-3	2-1/2% Cold-leg break	7, 8[a]
S-UT-6	5% Cold-leg break	9, 10, 11[a]
S-UT-7	5% Cold-leg break with UHI	9, 10, 11[a]
S-NC-2B	Natural-circulation, single-, two-phase, reflux	12[a]
S-NC-3	Natural-circulation, two-phase	12[a]
S-NC-8B	Natural-circulation, reflux	*a*
S-UT-8	Repeat of S-UT-6 with modified guide tube	13[a]
S-IB-1	100% Cold-leg break, survival test for RVLIS	*b*
SC-WSPT-20	Frequency response test of RVLIS	14

[a]NOTE: Data for analysis were obtained from NRC Data Bank via phone line hookup.

[b]Informal transmission of data from W. W. Tingle (Idaho National Engineering Laboratory) to G. N. Miller (ORNL).

6. The Westinghouse RVLIS survived an intermediate-break test (S-IB-1) and was able to produce trending information after the blowdown. For the tests at Semiscale the RVLIS did not produce any measurements that were ambiguous as to the coolant level. The RVLIS does not measure the coolant level but rather the collapsed liquid level. In all the testing at Semiscale the collapsed liquid level was lower than or equal to the coolant (two-phase froth) level. This condition is expected to be true for PWRs.

REFERENCES

1. G. N. Miller et al., "High Temperature, High Pressure Water Level Sensor," pp. 877-81 in *IEEE Ultrasonics Symposium Proceedings*, Vol. 2, Cat. No. 80CH1602-2, October 1980.

2. *NRC Action Plan Developed as a Result of the TMI-2 Accident*, NUREG-0660, Sects. 1.D.5 and 2.F.2 (May 1980).

3. *TMI-2 Lessons Learned Task Force Status Report and Short-Term Recommendation*, NUREG-0578, pp. A-11-12 (July 1979).

4. K. G. Turnage et al., *Advanced Two-Phase Flow Instrumentation Program Quart. Prog. Rep. for July-September 1980*, NUREG/CR-1903 (ORNL/NUREG/TM-430).

5. K. G. Turnage et al., *Advanced Two-Phase Flow Instrumentation Program Quart. Prog. Rep. for October-December 1980*, NUREG/CR-2007 (ORNL/NUREG/TM-443).

6. J. E. Hardy et al., *Advanced Two-Phase Flow Instrumentation Program Quart. Prog. Rep. for April-June 1981*, NUREG/CR-2204, Vol. 2 (ORNL/NUREG/TM-8010).

7. J. E. Hardy et al., *Advanced Two-Phase Flow Instrumentation Program Quart. Prog. Rep. for July-September 1981*, NUREG/CR-2204, Vol. 3 (ORNL/NUREG/TM-8162).

8. J. E. Hardy et al., *Advanced Two-Phase Flow Instrumentation Program Quart. Prog. Rep. for October-December 1981*, NUREG/CR-2204, Vol. 4 (ORNL/NUREG/TM-8231).

9. N. S. Tsannes, "Joule and Wiedemann Effects - The Simultaneous Generation of Longitudinal and Torsional Stress Pulses in Magnetostrictive Materials," *IEEE Transactions on Sonics and Ultrasonics*, Vol. SU-13, No. 2, pp. 33-41 (July 1966).

10. S. Spinner and R. C. Valore, "Comparison of Theoretical and Empirical Relations Between the Shear Modulus and Torsional Resonance Frequencies for Bars of Rectangular Cross Section," *J. Natl. Bur. Std.*, 60(5), Research Paper 2861 (May 1958).

11. L. C. Lynnworth, "Slow Torsional Wave Sensors," pp. 29 34 in *IEEE Ultrasonics Symposium Proceedings*, Cat. No. 77CH1264-ISU (1977).

12. S. Davidson, "Wire and Strip Delay Lines," *Ultrasonics*, July-September 1966.

13. J. E. Hardy and G. N. Miller, *Analysis of the Performance of the Westinghouse Reactor Vessel Indicating System for Tests at SEMISCALE*, NUREG/CR-2720 (ORNL/NUREG/TM-8336) (to be published).

NUREG/CR-2752, Vol. 1
ORNL/TM-8365
Dist. Category R2

Internal Distribution

1. J. L. Anderson
2. R. L. Anderson
3. S. K. Combs
4. W. G. Craddick
5. J. E. Hardy
6. H. W. Hoffman
7. A. F. Johnson
8. T. S. Kress
9. A. L. Lotts
10. G. N. Miller
11. F. R. Mynatt

12-13. T. W. Robinson, Jr.
14. S. C. Rogers
15. J. A. Stevens
16. D. G. Thomas
17. H. E. Trammell
18. W. L. Zabriskie
19. ORNL Patent Office
20. Central Research Library
21. Document Reference Section
22-23. Laboratory Records Department
24. Laboratory Records (RC)

External Distribution

25. C. W. Connell, Jr., Babcock & Wilcox, Nuclear Power Generation Division, Lynchburg, VA 24505
26. R. E. Bryan, Combustion Engineering, 1000 Prospect Hill Road, Windsor, CT 06095
27. W. G. Lyman, Westinghouse Electric Company, Monroeville Nuclear Center, P.O. Box 355, Pittsburgh, PA 15230

28-35. Director, Division of Accident Evaluation, Nuclear Regulatory Commission, Washington, D.C. 20555
36. Director, Reactor Division DOE, ORO, Oak Ridge, TN 37830
37. Office of Assistant Manager for Energy Research and Development, DOE, ORO, Oak Ridge, TN 37830

38-42. Director, Reactor Safety Research Coordination Office, DOE, Washington, D.C. 20555
43. H. D. Wills, General Electric, 175 Curtner St., MC 214, San Jose, Ca 94303
44. P. G. Bailey, Electric Power Research Institute, P.O. Box 10412, Palo Alto, Ca 94303

45-46. Technical Information Center, DOE, Oak Ridge, TN 37830
47-391. Given distribution as shown in category R2 (10-NTIS)
392-429. Special NRC External Distribution

120555078877 1 ANR2
US NRC
ADM DIV OF TIDC
POLICY & PUBLICATIONS MGT BR
PDR NUREG COPY
LA 212
WASHINGTON DC 20555